International Journal of Mechanical, Industrial and Aerospace Sciences
ISSN: 2517-9950
Vol:8, No:6, 2014

Surface Roughness Effects in Pure Sliding EHL Line Contacts with Carreau-Type Shear-Thinning Lubricants

Punit Kumar, Niraj Kumar

***Abstract*—**The influence of transverse surface roughness on EHL characteristics has been investigated numerically using an extensive set of full EHL line contact simulations for shear-thinning lubricants under pure sliding condition. The shear-thinning behavior of lubricant is modeled using Carreau viscosity equation along with Doolittle-Tait equation for lubricant compressibility. The surface roughness is assumed to be sinusoidal and it is present on the stationary surface. It is found that surface roughness causes sharp pressure peaks along with reduction in central and minimum film thickness. With increasing amplitude of surface roughness, the minimum film thickness decreases much more rapidly as compared to the central film thickness.

***Keywords*—**EHL, Carreau, Shear-thinning, Surface Roughness, Amplitude, Wavelength.

I. Introduction

THE heavily loaded line contacts involved in mechanical components such as gears, cams and roller bearings often operate within elastohydrodynamic lubrication (EHL) regime. This mode of hydrodynamic lubrication is characterized with significant elastic deformation of interacting surfaces and increase in lubricant viscosity due to extremely high contact pressure. Owing to the complexities involved in an EHL problem, the prediction of EHL characteristics has been the subject of extensive study over the last six decades. For an accurate and reliable a prediction, it becomes necessary to consider the effects of realistic lubricant rheology and surface roughness.

Earlier EHL studies [1], [2] were based on the assumption of Newtonian fluid model which assumes a constant value of viscosity, whereas, it is well established that the EHL lubricants (such as polymer thickened mineral oils and synthetic oils) exhibit considerable shear-thinning, i.e., loss of effective viscosity at high shear stress. This causes significant reduction in EHL film thickness. Therefore, several EHL studies [3]-[20] employing different shear-thinning models are available in the literature. For instance, the sinh-law, often referred as Ree-Eyring model, has been the most widely used rheological model [3], [6]. Recently, Bair [10] presented strong evidence from the original published works of Henry Eyring that sinh-law was not intended for characterizing shear-thinning fluids [11]. The actual Ree-Eyring model was employed by Kumar et al. [12] in full EHL line and point contact simulations to obtain film thickness values in close agreement with experimental data. Recent studies [13]-[15] have demonstrated that the shear-thinning behavior exhibited by EHL lubricants is best modeled by power-law based Carreau-type viscosity models. Using this model, good agreement with experimental date has been reported.

As mentioned earlier, surface roughness also plays an important role in elastohydrodynamic lubrication. It causes very high localized pressures at the asperity tips which may lead to direct metal-metal contact and hence, failure. Therefore, several attempts have been made in order to model the effects of surface roughness on EHL characteristics.

In particular, a flow-factor method based upon an average Reynolds equation was introduced by Patir and Cheng [16] to account for the effect of fluid flow past the rough surfaces. While originally developed for hydrodynamic lubrication, this method was widely applied in EHL investigations as well [17], [18]. However, it was realized that the flow factor method has some serious shortcomings. Therefore, a micro-EHL [19], [20] approach was introduced which involved the modification of film thickness equation to include the term pertaining to the geometry and motion of surface irregularities in the EHL contact. Lubrecht et al. [21] and Kweh et al. [22] also used this approach to analyze EHL contacts of wavy surfaces under steady-surface condition with single sinusoidal wave. Venner and Napel [23] employed a deterministic description of an actually measured surface roughness profile in EHL line contacts simulations using Newtonian fluid model. Chang and Webster [24] reported much smaller pressure ripples in rolling contacts as compared to those in sliding contacts.

Chang et al. [25] presented a micro-EHL analysis which included the effects of shear-thinning behavior. Similarly, Kumar et al. [26] incorporated the effect of sinusoidal surface rough in EHL analyses.

Most of the available studies on the combined effects of surface roughness and shear-thinning behavior are based upon unrealistic rheological and piezo-viscous models. Therefore, the present paper aims at studying the finer aspects related to the influence of lubricant rheology on EHL characteristics of rough line contacts under pure sliding. The most realistic Carreau shear-thinning model has been used along with Doolittle-Tait piezo-viscous relationship.

Punit Kumar is with the Department of Mechanical Engineering, National Institute of Technology, Kurukshetra, Haryana, India-136119 (Phone: 91-8059000776, e-mail: punkum2002@yahoo.co.in).

Niraj Kumar is also with the Department of Mechanical Engineering, National Institute of Technology, Kurukshetra, Haryana, India-136119 (Phone: 91-1744-233447, e-mail: niraj_me01336@yahoo.com).

II. Governing Equations

A. Shear-Thinning Model

The generalized viscosity (η) is obtained using the following Carreau shear-thinning model:

$$\eta = \tau / \dot{\gamma} = \mu \left[1 + \left(\frac{\mu \dot{\gamma}}{G_{cr}} \right)^2 \right]^{\frac{(n-1)}{2}} \tag{1}$$

where, μ is the low-shear viscosity. $\dot{\gamma} = \partial u / \partial y$ is the shear rate, n is the power-law index and G_{cr} is a critical stress representing the Newtonian limit of lubricants.

B. Generalized Reynolds Equation

The dimensionless generalized Reynolds equation for the case of EHL line contact is:

$$\frac{\partial}{\partial X}\left(\bar{\rho} H^3 \bar{F}_2 \frac{\partial P}{\partial X} \right) = K \frac{\partial}{\partial X}(\bar{\rho} H) + K \frac{S}{2} \frac{\partial}{\partial X}\left[\bar{\rho} H \left(1 - 2 \frac{\bar{F}_1}{\bar{F}_0} \right) \right] \tag{2}$$

where $X = \frac{x}{b}$, $P = \frac{p}{p_H}$, $\bar{\rho} = \frac{\rho}{\rho_o}$, $K = U \left(\frac{\pi}{4W} \right)^2$ and $S = \frac{(u_2 - u_1)}{u_o}$

The integral functions used in the Reynolds (2) are defined as follows:

$$\bar{F}_0 = \int_0^1 \frac{1}{\bar{\eta}} dY, \; \bar{F}_1 = \int_0^1 \frac{Y}{\bar{\eta}} dY \text{ and } \bar{F}_2 = \int_0^1 \frac{Y}{\bar{\eta}} \left(Y - \frac{\bar{F}_1}{\bar{F}_0} \right) dY \tag{3}$$

where $Y = y / h$ and $\bar{\eta} = \eta / \mu_o$

Boundary conditions

$$P = 0 \text{ at } X = X_{in} \tag{4}$$

$$P = \frac{\partial P}{\partial X} = 0 \text{ at } X = X_o \tag{5}$$

C. Film Thickness Equation

$$H(X) = H_o + \frac{X^2}{2} + \frac{1}{\pi} \sum_{j=1}^{N} D_{ij} P_j + A \sin\left(2\pi X / \bar{\lambda} \right) \tag{6}$$

where A and $\bar{\lambda}$ are the dimensionless amplitude and wavelength of surface roughness respectively and D_{ij} are the influence coefficients:

$$D_{ij} = -\left(i - j + \frac{1}{2} \right) \Delta X \left[\ln\left(\left| i - j + \frac{1}{2} \right| \Delta X \right) - 1 \right] + \left(i - j - \frac{1}{2} \right) \Delta X \left[\ln\left(\left| i - j - \frac{1}{2} \right| \Delta X \right) - 1 \right] \tag{7}$$

D. Density-Pressure Relationship

The Tait's equation of state is used here to represent lubricant compressibility:

$$\frac{\rho_o}{\rho} = \frac{V}{V_o} = 1 - \frac{1}{1 + K_o'} \ln\left[1 + \frac{p}{K_o} \left(1 + K_o' \right) \right] \tag{8}$$

E. Viscosity- Pressure Relationship

The following Doolittle free volume equation is used here:

$$\mu = \mu_o \exp\left(B \frac{V_\infty}{V_o} \left[\frac{1}{\frac{V}{V_o} - \frac{V_\infty}{V_o}} - \frac{1}{1 - \frac{V_\infty}{V_o}} \right] \right) \tag{9}$$

The representative values assigned to the Doolittle and Tait parameters are listed in Table I.

TABLE I
Doolittle And Tait Parameters

B	V_∞ / V_o	K'	K_o /GPa
4.325	0.6669	10.859	0.9159

F. Load Equilibrium Equation

$$\int_{X_{in}}^{X_o} P dX = \frac{\pi}{2} \tag{10}$$

III. Solution Procedure

The solution domain ($-4 \le X \le 1.5$) is discretized using a uniform mesh with a grid size of ΔX = 0.01. Further mesh refinement is found to cause negligible change in the results. As outlined by Kumar and Anuradha [15], the procedure consists of the following steps:

1. The solution begins by assuming an initial guess for the pressure distribution $[P_i]$ and offset film thickness H_o.
2. The film profile $[H_i]$ is calculated using the pressure distribution $[P_i]$ in the film thickness (6).
3. The fluid density (ρ) and viscosity (μ_1) are calculated using (8) and (9), respectively.
4. The valuE of $\bar{\eta}$ defined by (1) is obtained iteratively.
5. The Reynolds Equation (1) is discretized to obtain the equations $f_i = 0$ (i=2 to N) as follows:

$$f_i = \varepsilon_{i+1/2} \frac{P_{i+1} - P_i}{\Delta X^2} - \varepsilon_{i-1/2} \frac{P_i - P_{i-1}}{\Delta X^2} - K \frac{\left[(\bar{\rho} H \omega)_i - (\bar{\rho} H \omega)_{i-1} \right]}{\Delta X} \tag{11}$$

where $\varepsilon_i = \bar{\rho}_i \left(\bar{F}_2 \right)_i H_i^3$ and $\omega_i = 1 + \frac{S}{2} \left(1 - 2 \frac{\bar{F}_1}{\bar{F}_0} \right)_i$

6. The load equilibrium (10) is written in the following discrete form using Simpson's coefficients:

$$\Delta W = \sum_{j=2}^{N} C_j P_j - \frac{\pi}{2} = 0 \tag{12}$$

where

$$C_j = \begin{cases} \Delta X/3 & j = N \\ 4\Delta X/3 & j = 2,4,6..... \\ 2\Delta X/3 & j = 3,5,7..... \end{cases} \quad (13)$$

7. The simultaneous system of N equations is solved using the Newton-Raphson technique [14]:

$$\begin{bmatrix} \frac{\partial f_2}{\partial P_2} & \frac{\partial f_2}{\partial P_3} & ..... & \frac{\partial f_2}{\partial P_N} & \frac{\partial f_2}{\partial H_0} \\ \frac{\partial f_3}{\partial P_2} & \frac{\partial f_3}{\partial P_3} & ..... & \frac{\partial f_3}{\partial P_N} & \frac{\partial f_3}{\partial H_0} \\ ..... & ..... & & ..... & ..... \\ ..... & ..... & & ..... & ..... \\ \frac{\partial f_N}{\partial P_2} & \frac{\partial f_N}{\partial P_3} & ..... & \frac{\partial f_N}{\partial P_N} & \frac{\partial f_N}{\partial H_0} \\ C_2 & C_3 & ..... & C_N & 0 \end{bmatrix} \begin{bmatrix} \Delta P_2 \\ \Delta P_3 \\ ..... \\ ..... \\ \Delta P_N \\ \Delta H_0 \end{bmatrix} = - \begin{bmatrix} f_2 \\ f_3 \\ ... \\ .... \\ f_N \\ \Delta W \end{bmatrix} \quad (14)$$

The pressure distribution $[P_i]$ and offset film thickness are updated using the correction calculated above.

8. The steps 2-8 are repeated until the following convergence criteria (15) and (16) are satisfied:

$$\frac{\left\| \left[\sum_{i=1}^{N} P_i \right]_n - \left[\sum_{i=1}^{N} P_i \right]_{n-1} \right\|}{\left\| \left[\sum_{i=1}^{N} P_i \right]_{n-1} \right\|} \le 10^{-5}, \quad (15)$$

$$\left| \frac{[H_o]_n - [H_o]_{n-1}}{[H_o]_{n-1}} \right| \le 10^{-4} \quad (16)$$

IV. Results and Discussion

The EHL model and the solution procedure described in the previous sections are applied for the evaluation of EHL characteristics in pure sliding line contacts. The values of various input parameters, unless stated otherwise, are taken from Table II.

TABLE II
Input Parameters

Inlet viscosity, μ_o	3.45 Pa-s
Power law index, n	0.65
Inlet viscosity, G_{cr}	5400 Pa
Inlet density, ρ_o	864 kg/m^3
Pressure -viscosity coefficient, α	2.83×10^{-8} Pa^{-1}
Equivalent radius of the disks, R	0.02 m
Equivalent elastic modulus, E'	2.1×10^{11} Pa

A. Effect of Roughness Amplitude

Figs. 1 (a) and (b) compare the pressure distributions and film shapes respectively, obtained for smooth (a=0) and rough surfaces (a=40nm and 80nm) with the roughness wavelength fixed at λ =40 μm.

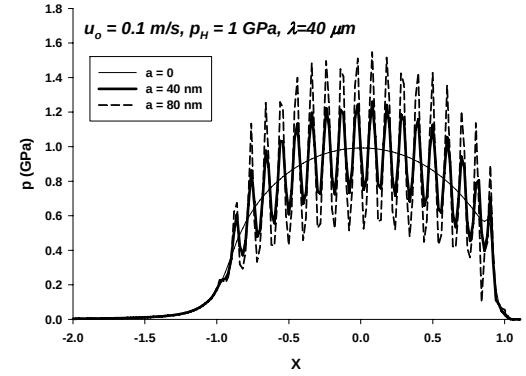

(a)

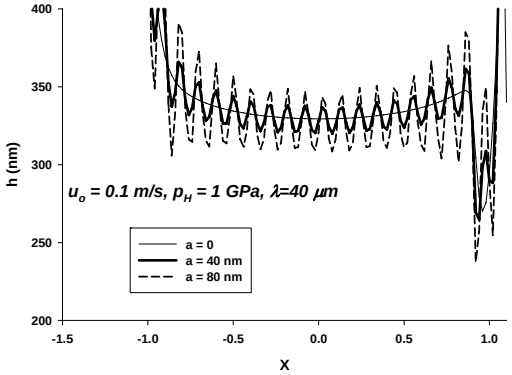

(b)

Fig. 1 (a) Pressure distributions and (b) Film shapes for smooth and rough surfaces

It can be seen that surface roughness causes ripples or localized pressure peaks at the asperity tips and the amplitude of these ripples increases with increasing amplitude of surface roughness. This is due to the fact that surface roughness offers resistance to fluid flow and hence, the hydrodynamic pressure rises locally in order to maintain the continuity of flow. Higher is the roughness amplitude, greater is the flow resistance and hence, more pronounced pressure rippling.

Figs. 2 (a) and (b) show the variation of central and minimum film thickness values respectively, with increasing amplitude of surface roughness. As apparent from this figure, surface roughness causes a reduction in EHL film thickness and the minimum film thickness undergoes a much larger reduction as compared to the central film thickness. The decrease in minimum film thickness is attributed to higher negative pressure gradient at the outlet for the case of rough surfaces as compared to that for smooth surface.

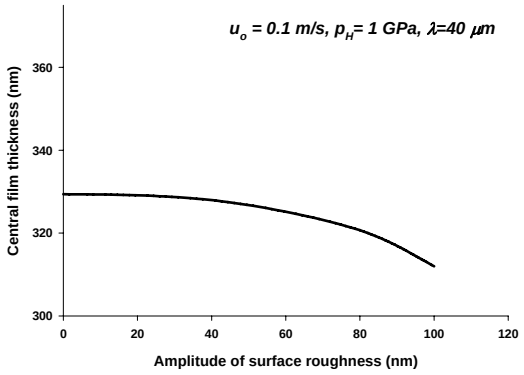

(a)

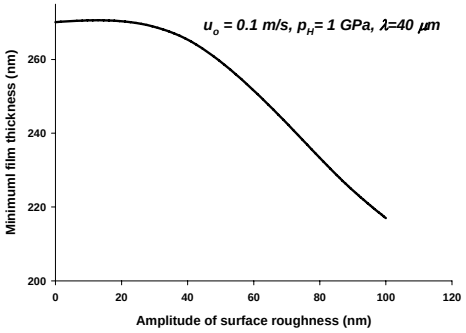

(b)

Fig. 2 Variation of (a) central and (b) minimum film thickness with roughness amplitude

B. Effect of Roughness Wavelength

In order to study the effect of roughness wavelength, Figs. 3 (a) and (b) compare the pressure distributions and film shapes respectively, for λ=40μm and 80μm with the roughness amplitude fixed at a=40nm. It can be seen that surface roughness with shorter wavelength causes more pronounced pressure ripples. This is attributed to greater flow resistance offered by asperities with sharper tips.

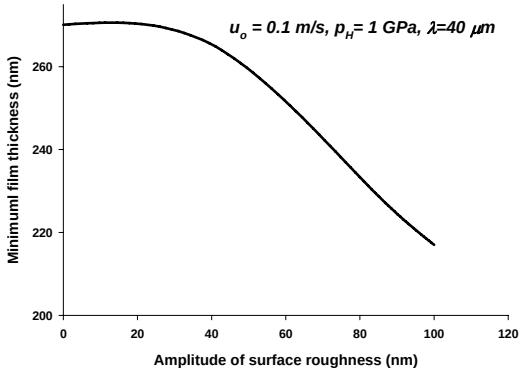

(a)

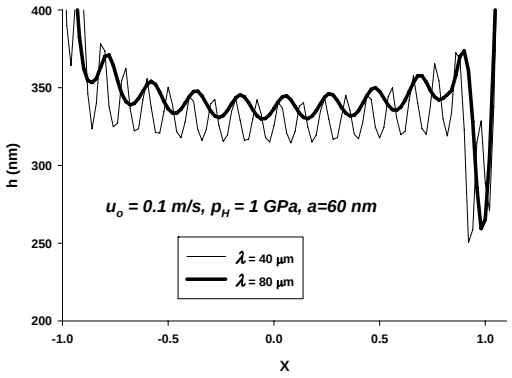

(b)

Fig. 3 (a) Pressure distributions and (b) Film shapes for different values of roughness wavelength

Figs. 4 (a) and (b) show the variation of central and minimum film thickness values respectively, with increasing wavelength of surface roughness. It can be seen that both central and minimum film thickness decrease with decreasing wavelength. It is quite interesting to note that the central film thickness increases above its smooth surface value at longer wavelengths of surface roughness. However, the minimum film thickness approaches smoothly towards its smooth surface value without overshooting it.

In other words, surface roughness with longer wavelength influences EHL film thickness to a lesser extent. Therefore, the machining process parameters should be controlled so as to minimize short wavelength component in surface topography. This will ensure lower pressure peaks at the asperity tips as well as lower reduction in film thickness. Needless to mention that a large reduction in EHL film thickness due to surface roughness may lead to metal-metal contact leading to excessive friction and wear. This behavior is taken into account using the Carreau shear-thinning model in the present analysis. However, it is a common practice to assume the lubricant to be Newtonian within the inlet zone. This may lead to significant errors.

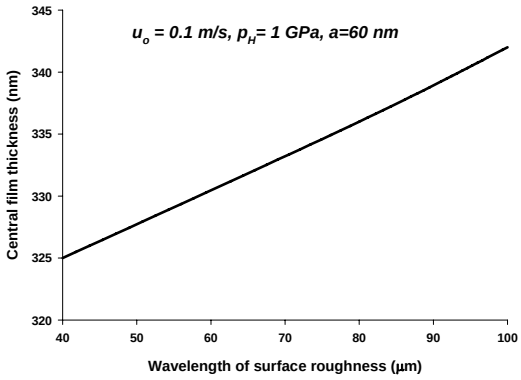

(a)

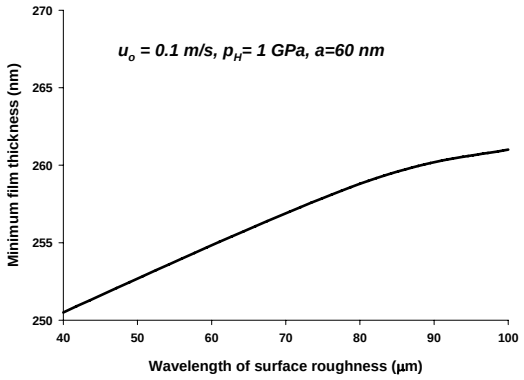

(b)

Fig. 4 Variation of (a) central and (b) minimum film thickness with roughness wavelength

In order to illustrate this, Fig. 5 compares the film shapes obtained using Newtonian and non-Newtonian fluid models. It can be seen from this figure that the EHL film for the case of non-Newtonian fluid is much thinner as compared to that for the Newtonian case. Therefore, as mentioned above, the use of Newtonian fluid model leads to overestimation of film thickness which may be quite dangerous if the lubricant is highly shear-thinning as in the present case. Therefore, it is necessary to measure the rheological properties of EHL lubricants accurately and employ realistic rheological models in EHL simulations.

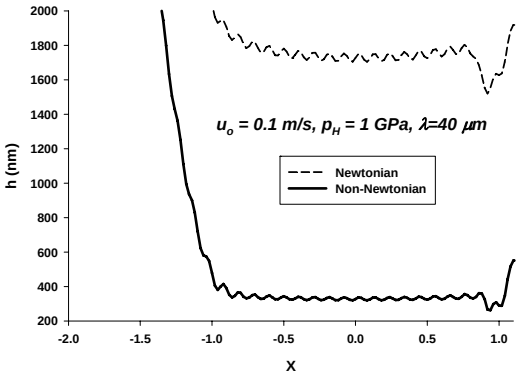

Fig. 5 Comparison of Film Profiles

V. Conclusions

The effect of surface roughness on EHL characteristics has been investigated using an extensive set of full EHL line contact simulations for shear-thinning lubricants under pure sliding condition. The lubricant rheology is described by Carreau shear-thinning model. It is found that surface roughness causes sharp pressure peaks along with reduction in central and minimum film thickness. With increasing amplitude of surface roughness, the minimum film thickness decreases much more rapidly as compared to the central film thickness. The effect of surface roughness on pressure profile and film thickness diminishes with increasing wavelength of roughness profile.

Nomenclature

Dimensional Parameters

b : half width of Hertzian contact zone (m**)**
E' : effective elastic modulus of rollers 1 and 2 (Pa).
h : film thickness (m)
p : Pressure (Pa)
p_H : maximum Hertzian pressure, (Pa)
R : equivalent radius of contact (m).
u_o : average rolling speed, $u_o = (u_1 + u_2)/2$, (m/s)
u_1, u_2 : velocities of lower and upper surfaces, (m/s)
w : applied load per unit length for line contact (N/m)

Greek symbols:

$\dot{\gamma}$: shear strain rate across the fluid film, (s^{-1})
ρ_o : inlet density of the lubricant (kg/m^3)
ρ : lubricant density at the local pressure (kg/m^3)
μ_o : inlet viscosity of the Newtonian fluid (Pa.s)
η : generalized Newtonian viscosity (Pa.s)

Dimensionless Parameters

H : dimensionless film thickness, $H = hR/b^2$
H_o : dimensionless offset film thickness,
P : dimensionless pressure, $P = p/p_h$
S : slide to roll ratio, $S = (u_2 - u_1)/u_o$
U : dimensionless speed parameter, $U = \dfrac{\mu_o u_o}{E'R}$
W : dimensionless load parameter, for line contact

References

[1] Dowson, D. and Higginson, G. R., 1966, Elastohydrodynamic lubrication: The Fundamentals of Roller and Gear Lubrication, Pergamon Press, Oxford.
[2] Hamrock, B. J. and Dowson, D., 1981, Ball bearing lubrication – The elastohydrodynamics of elliptical contacts, John Wiley & Sons.
[3] Hirst, W. and Moore, A. J., 1974, "Non-Newtonian Behavior in Elastohydrodynamic Lubrication," Proc. Roy. Soc. London, Series A, vol. 337, p. 101.
[4] Johnson, K. L. and Tevaarwerk, J. L., 1977, "Shear behavior of EHD Oil Films," Proc. Roy. Soc. London, Series A, vol. 356, pp. 215-236.
[5] Conry, T. F., Wang, S. and Cusano, C., 1987, "A Reynolds-Eyring Equation for Elastohydrodynamic Lubrication in Line Contacts," ASME Journal of Tribology, vol. 107, pp. 648-658.
[6] Chang, L., Cusano, C. and Conry, T. F., 1988, " Effects of Lubricant Rheology and Kinematic Conditions Micro-Elastohydrodynamic Lubrication," ASME Journal of Tribology, vol. 111, p. 344.
[7] Evans, C. R. and Johnson, K. L., 1986, "The Rheological Properties of Elastohydrodynamic Lubrication," Proc. Instn. Mech. Engr., vol. 200, No. C5, pp. 301-312.
[8] Bair, S. and Winer, W. O., 1979, "A Rheological Model for Elastohydrodynamic Contacts Based in Primary Laboratory Data," ASME Journal of Lubrication Technology, vol. 101, No. 3, pp. 258-265.
[9] Lee, R. T. and Hanrock, B. J., 1990, "A Circular Non-Newtonian Fluid

Model: Part I-Used in Elastohydrodynamic Lubrication," ASME Journal of Tribology, vol. 112, pp. 486-496.
[10] Bair, S., 2004, "Actual Eyring Models for Thixotropy and Shear-Thinning: Experimental Validation and Application to EHD," ASME Journal of Tribology, vol. 126, pp.728-732
[11] Ree, F. H., Ree, T. and Eyring, H., 1958, "Relaxation Theory of Transport Problems in Condensed Systems," Ind. Eng. Chem., vol. 50, pp. 1036-1038.
[12] Kumar, P., Khonsari, M. M. and Bair, S., 2009, "Full EHL Simulations Using the Actual Ree-Eyring Model for Shear Thinning Lubricants," ASME Trans. Journal of Tribology, vol.131, pp. 011802-1-6.
[13] Jang, J.Y., Khonsari, M. M., Bair, S., 2007, "On the elastohydrodynamic analysis of shear-thinning fluids," Proceeding of Royal Society (London) vol. 463, pp. 3271-3290.
[14] Kumar, P. and Khonsari, M. M., 2008, "Combined effects of shear thinning and viscous heating on EHL characteristics of rolling/sliding line contact" ASME Trans. J. Tribol., vol. 130, pp. 041505-1-13.
[15] Anuradha, P. and Kumar, P., 2011, "New Film Thickness Formula for Shear Thinning Fluids in Thin Film EHL Line Contacts", Proc. IMechE, Part J, vol. 225, pp. 173-179.
[16] Patir, N and Cheng, H. S., 1978, "An Average Flow Model for Determining the Effects of Three-Dimensional Roughness on Partial Hydrodynamic Lubrication," ASME Journal of Tribology, vol. 100, pp. 12-17.
[17] Phan-Thien, N., 1982 "On the Mean Reynolds Equation in the Presence of Homogeneous Random Surface Roughness," ASME Journal of Applied Mechanics, vol. 49, pp. 476-480.
[18] Sadeghi, F., and Sui, P. C., 1989, "Compressible Elastohydrodynamic Lubrication of Rough Surfaces, ASME Journal of Tribology, vol. 111, pp. 56-62.
[19] Chang, L., Cusano, C. and Conry, T. F., 1988, " Effects of Lubricant Rheology and Kinematic Conditions Micro-Elastohydrodynamic Lubrication," ASME Journal of Tribology, vol. 111, p. 344.
[20] Ai, X. and Zheng, L., 1989 "A General Model for Microelastohydrodynamic Lubrication and its Full Numerical Solution," ASME Journal of Tribology, vol. 111, No. 4, pp. 569-576.
[21] Lubrecht, A. A., ten Napel, W. E. and Bosma, R., 1989, "The Influence of Longitudinal and Transverse Roughness on Elastohydrodynamic Lubrication of Circular Contacts," ASME Journal of Tribology, vol. 110, No. 3, pp. 421-426.
[22] Kweh, C. C., Patching, M. J., Evans, H. P. and Snidle, R. W., 1992, "Simulation of Elastohydrodynamic Contacts Between Rough Surfaces," ASME Journal of Tribology, vol. 114, pp. 412-419.
[23] Venner, C. H., and Napel, W. E. ten, 1992, "Surface Roughness Effects in EHL Line Contacts," ASME Journal of Tribology, vol. 114, pp. 616-622.
[24] Chang, L. and Webster, M. N., 1991, "A Study of Elastohydrodynamic Lubrication of Rough Surfaces," ASME Journal of Tribology, vol. 113, pp. 110-115.
[25] Chang, L. Webster, M. N., and Jackson, A.,1993, "On the Pressure Rippling and Roughness Deformation in Elastohydrodynamic Lubrication of Rough Surfaces," ASME Journal of Tribology, vol. 115, pp. 439-444.
[26] Kumar, P., Jain, S. C. and Ray, S., 2002, "Thermal EHL of Rough Rolling/Sliding Line Contacts Using a Mixture of Two Fluids at Dynamic Loads," ASME Trans. Journal of Tribology, vol. 124, pp. 709-715.